Quantum Correlated Neutrosophic Extreme Machine Learning with Chromosomal Abnormality for Down Syndrome Diagnosis

S. Jesmitha
Department of ECE, School of Engineering, JAIN University, Bangalore, India
jesmitha.n@gmail.com (corresponding author)

T. R. Manjula
Department of ECE, School of Engineering, JAIN University, Bangalore, India
Tr.manjula@jainuniversity.ac.in

Received: 21 February 2026 | Revised: 16 March 2026 and 2 April 2026 | Accepted: 17 April 2026

 DOI: https://doi.org/10.48084/etasr.18297

ABSTRACT

Down Syndrome (DS), caused by the presence of a third copy of chromosome 21, is the most common form of aneuploidy. Prenatal screening for DS has become an essential component of modern antenatal healthcare, enabling early detection of chromosomal abnormalities during pregnancy. This study presents an accurate prenatal diagnostic procedure for DS with minimal misclassification. Over the past few years, Machine Learning (ML) has gained significant attention in predictive analytics for medical applications. However, its applications in DS diagnosis remain limited due to the challenges associated with highly correlated screening features. This study presents a method called Quantum Correlated Neurotrosophic Extreme Machine Learning (QC-NEML) for prenatal diagnosis and identification of chromosomal abnormalities associated with DS. First, Quantum Correlated-based feature extraction is used to extract the most significant features in determining DS. The extracted features are then used in a Neutrosophic Extreme ML-based model for prenatal diagnosis and identification of DS chromosomal abnormalities. The proposed QC-NEML method was evaluated using precision, recall, accuracy, and misclassification rate, achieving higher performance compared to other state-of-the-art methods on a Chromosome karyotype image dataset, illustrating its effectiveness in reducing misclassification rate while significantly improving overall accuracy.

Keywords-Down syndrome; prenatal diagnosis; quantum correlated; neurotrosophic machine learning

I. INTRODUCTION

Down Syndrome (DS), also known as trisomy 21, is one of the most common chromosomal disorders worldwide that occurs due to the presence of an additional copy of chromosome 21, leading to developmental and intellectual impairments. The most prominent characteristics of SD include intellectual disability and craniofacial dysmorphisms. DS occurs in approximately 1 in 1000 births worldwide.

The integration of Artificial Intelligence (AI) into chromosomal karyotyping analysis represents a significant advance that can improve diagnostic speed and accuracy [1, 2]. In [1], three different combinations of ML prediction methods for screening of DS in the first and second trimesters were presented, with the XGBoost model achieving the best prediction performance. In [3], a review of traditional methods and sequencing techniques for the detection of DS in the early stages was presented. In [4], Elephant Herd Whale Optimization and Stacked ResNet-Bidirectional Long Term Short Memory (ResNet-BiLSTM) were employed to improve the detection and classification of genetic disorders. Previous studies have also conducted comprehensive surveys on prenatal diagnostic techniques for identifying fetal abnormalities using clinical and computational methods [5]. In [6], a detailed cytogenetic analysis was presented for the accurate detection of DS.

In [7], the screening for DS in the second trimester was retrospectively analyzed, and an ML method based on Random Forest was developed to predict DS, but the training time was not considered. In [8], a holistic approach took into account the genetic mechanisms and cognitive impairments of DS, but positive-negative classification rates were not analyzed. Recent studies, such as [9], have applied deep learning techniques, particularly Convolutional Neural Networks (CNNs), for chromosome image analysis and genetic disorder detection. Architectures such as ResNet and VGG can automatically learn discriminative chromosome features for karyotype classification. However, these methods often require large annotated datasets and large amounts of computational resources.

The motivation in [10] was the application of ML mechanisms to provide an in-depth analysis of clinical records acquired from subjects with DS, and to validate their correlation results with test samples. In [11], a detailed literature survey was presented for both pregnancy care and maternal mortality reduction, while in [12], another overview of DS was introduced, focusing on its diagnosis and management. The method in [13] combined digital image analysis and supervised learning to quantify fat droplets in liver biopsy images for Non-Alcoholic Fatty Liver Disease (NAFLD), revealing that excluding unrelated histological features from calculations can lead to better results.

Many studies emphasize precision and recall but overlook overall accuracy and misclassification rates in diagnosing DS. To address this gap, this study developed a Quantum Correlated and Neurotrosophic Extreme ML-based (QC-NEML) prenatal diagnostic model to improve the accuracy of DS diagnosis, which focuses on efficient feature representation and is suitable for limited computing environments.

II. METHODOLOGY

DS is caused by genomic microduplications and dosage imbalances of human chromosome 21 and is associated with various genomic and phenotypic abnormalities. Globally, DS occurs in approximately 1 in 1,000 births, representing a significant prevalence, yet effective cures remain unavailable. Current strategies for managing DS primarily rely on screening and early detection. The proposed QC-NEML method is designed to extract richer information from chromosome karyotype images, enabling more robust and reliable chromosome classification. The proposed method consists of two steps: (1) Quantum Correlated (QC)-based Feature Extraction and (2) Neutrosophic Extreme ML (NEML) Classification for DS prediction. Figure 1 displays the proposed QC-NEML framework for DS prediction.

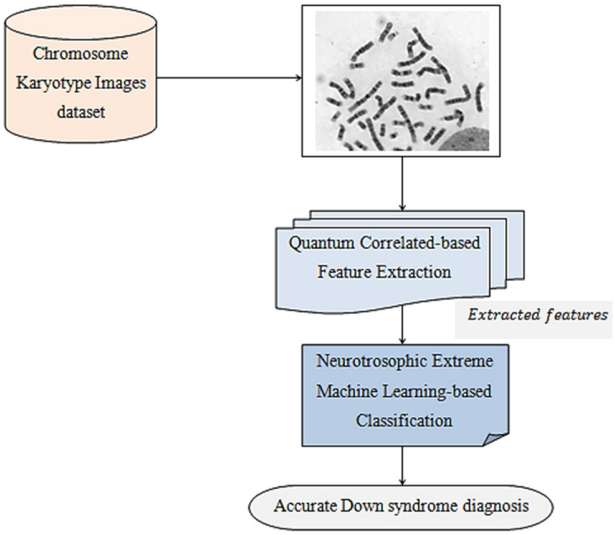

Fig. 1. Overall framework of the proposed QC-NEML model for prenatal DS diagnosis.

As shown in Figure 1, the chromosome karyotype image dataset is processed through two stages: feature extraction and classification. First, the most significant features in the chromosome karyotype images are extracted. Then, the extracted features are used as input to a Neutrosophic Extreme ML-based classification algorithm for the identification of DS chromosomal abnormalities.

III. DATASET DESCRIPTION

This study utilized the Chromosome Karyotype Images dataset [14] to detect chromosomal abnormalities and improve DS diagnosis. The images in this dataset were captured through a microscope camera with optimized focus and angles, while G-banding preparation involves culturing, staining, and metaphase arrest of amniotic cells. Karyotypes, interpreted per ISCN, represent the full chromosome set to identify numerical or structural abnormalities. G-banding provides detailed structural information, crucial for diagnosing genetic disorders such as trisomy 21 in DS. This combination ensures accurate prenatal detection. The similarity in size and banding patterns between chromosome pairs indicates the presence of DS. Autosome pairs are numbered and arranged from largest to smallest for analysis.

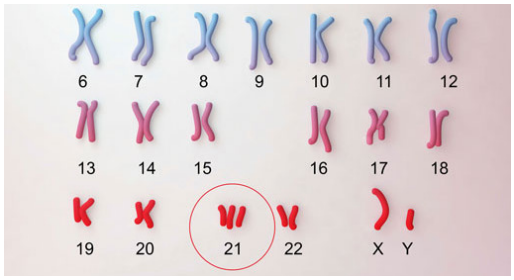

Fig. 2. Example chromosome karyotype image.

TABLE I. DATASET DESCRIPTION

	Chromosome karyotype images	Samples
1	Normal	4893
2	Number_abnormalities	57
3	Structural_abnormalities	50
Total		5000

As shown in Table I, a total of 5000 chromosome samples (3750 training and 1250 testing images) were used for training and validation.

IV. QUANTUM CORRELATED-BASED FEATURE EXTRACTION

The proposed feature extraction strategy is quantum-inspired rather than based on physical quantum computing hardware. QC-based feature extraction was applied using annotated chromosome images (Figure 3).

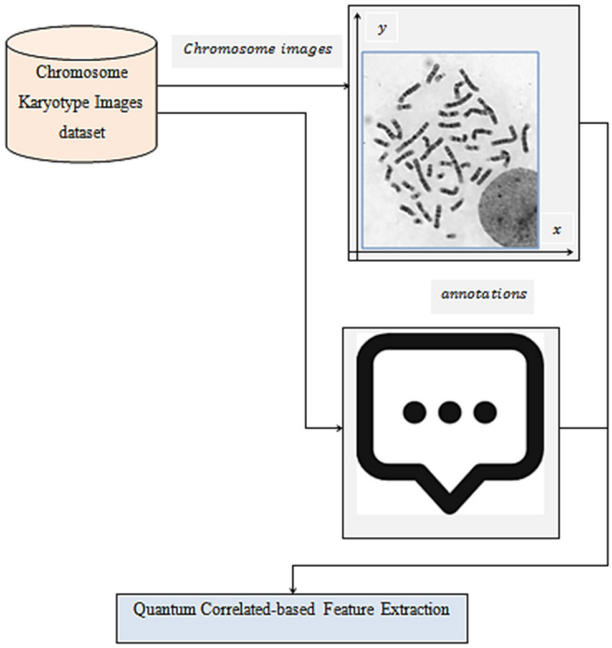

Fig. 3. Structure of chromosome images and annotations employed in the design of the QC-based feature extraction model.

In this approach, chromosome karyotype features are encoded using a qubit-inspired probabilistic representation. A qubit can represent two states simultaneously through probability amplitudes, allowing a compact representation of multiple correlated chromosome features. This representation enables modeling correlations among chromosome characteristics such as size, banding pattern, and bounding box coordinates within a unified probabilistic feature space. Unlike classical binary encoding, the qubit-based representation captures multi-state relationships between chromosome attributes, improving feature expressiveness for DS detection. Two types of alternative transformations, modeling x- and y-coordinates, are examined using binary states. Multi-objective optimization is applied to handle both transformations simultaneously without redundancy across the sample images.

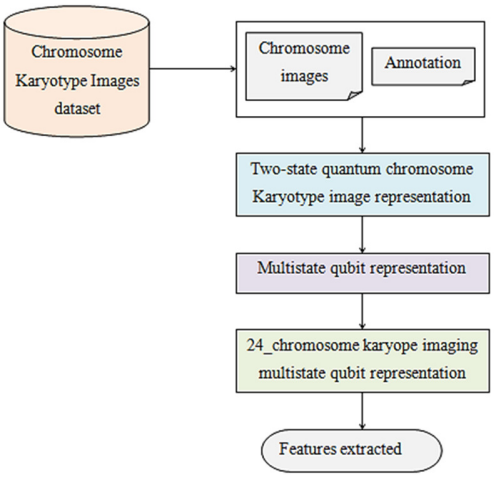

Fig. 4. Structure of QC-based feature extraction model.

Annotation files support analysis and validation, while feature-class correlations extract the most significant chromosomal features for DS detection. Unlike conventional methods, the model analyzes the entire chromosome set using QC-based feature extraction for precise abnormality detection. Qubits, representing 100 or 000 states, encode chromosome image information for processing, as shown in Figure 4.

A. Qubit Representation of Chromosome Features

In the proposed framework, chromosome karyotype features are represented using a quantum-inspired qubit encoding scheme. It should be noted that the proposed model does not require a physical quantum computer; instead, it adopts a quantum-inspired probabilistic representation to encode multiple chromosome attributes simultaneously. A qubit is mathematically represented as a superposition of two basis states:

$$|\psi_{state}| = \gamma|0> + \beta|1> \quad (1)$$

where: γ is the probability amplitude of state |0> and β is the probability amplitude of state |1>. The normalization condition is given by:

$$|\gamma|^2 + |\beta|^2 = 1$$

In the proposed model, chromosome image attributes such as size, bounding box coordinates, and banding patterns are mapped into binary states using feature normalization. These normalized values are then encoded into qubit amplitudes, allowing the chromosome features to be represented probabilistically. Each chromosome karyotype image is encoded as a qubit representing probabilities of normal, numerical, or structural abnormalities. A tertiary coding process is applied to handle these multistate qubits for accurate representation in the 24-chromosome karyotype. This is mathematically represented as

$$C_i^{(g)} = \begin{bmatrix} \gamma_1 & \gamma_2 & \dots & \gamma_m \\ \beta_1 & \beta_2 & \dots & \beta_m \end{bmatrix}, \quad |\gamma_1|^2 + |\beta_2|^2 = 1 \quad (2)$$

where $C_i^{(g)}$ denotes the 24 chromosome karyotype of the i-th sample in generation g, Q_j is the j-th qubit, and m=24 is the number of chromosomes

The three qubits representation for superposition of multiple states (i.e., 24-chromosome karyope imaging) is mathematically represented as:

$$|\psi_{state}| = \begin{bmatrix} \frac{1}{\sqrt{2}} & \frac{1}{\sqrt{2}} & \frac{1}{\sqrt{2}} \\ \frac{1}{\sqrt{2}} & -\frac{1}{\sqrt{2}}\frac{\sqrt{3}}{2} & \end{bmatrix} = \frac{1}{4}\left|000> + \frac{\sqrt{3}}{4}\right| 001 >$$

$$-\frac{1}{4}\left|010> - \frac{\sqrt{3}}{4}\right| 011 > + \frac{1}{4}\left|100> + \frac{\sqrt{3}}{4}\right| 101 >$$

$$-\frac{1}{4}\left|110> - \frac{\sqrt{3}}{4}\right| 111 > \quad (3)$$

This necessitates a three-qubit mechanism for storing extracted superpositions of multiple states:

3-qubit system = 2^3 = 8 states

These states correspond to different combinations of chromosome attributes extracted from the image annotations.

The features include chromosome name, width, height, depth, and bounding box coordinates (xmin, xmax, ymin, ymax). By encoding these attributes into a three-qubit superposition state, the model captures correlations among chromosome features within a compact representation space. The qubit representation assists in denoting the superposition of states and improves feature extraction for the identification of DS compared to the traditional methods. Here, only one of the 24-chromosome karyotype imaging is required to represent seven states, whereas in the case of traditional modeling, a minimum of seven chromosomes is required. The correlated results to analyze and validate different subsets (i.e., size and box) are mathematically formulated as:

$$[x] = FE\,[x] = \rho[PC(p,q)] = \frac{\Sigma_i(p_i-\mu_p)(q_i-\mu_q)}{\sqrt{\Sigma_i(p_i-\mu_p)^2}\sqrt{\Sigma_i(q_i-\mu_q)^2}} \quad (4)$$

where μ_x is the mean of size features and μ_y is the mean of bounding box features. μ_p and μ_q denote the mean value of 24-chromosome karyope imaging vectors p and q, respectively, with the resultant value of PC being $[-1,+1]$. The closer to $+1$, the higher the positive correlation, and the closer to -1, the higher the negative correlation. To measure abnormalities in the chromosomal karyotype, mean Average Precision (mAP) and mean Average Recall (mAR) are evaluated to designate a negative sample as positive and obtain all positive instances of each class, respectively, mathematically formulated as:

$$\mu AP = \frac{1}{N}\frac{\sum_{i=1}^{N} pixel_{i,i}}{\sum_{i=0}^{N}\sum_{j=1}^{N} pixel_{i,i}+pixel_{i,j}} \quad (5)$$

$$\mu AR = \frac{1}{N}\frac{\sum_{i=1}^{N} pixel_{i,i}}{\sum_{i=0}^{N}\sum_{j=1}^{N} pixel_{i,i}+pixel_{j,i}} \quad (6)$$

where the total number of output classes is N, $pixel_{i,i}$ represents the chromosomal karyotype pixels classified as class i and labeled as class i. In a similar manner, $pixel_{i,j}$ and $pixel_{j,i}$ represent the chromosomal karyotype pixels classified in class i but labeled class j and vice versa.

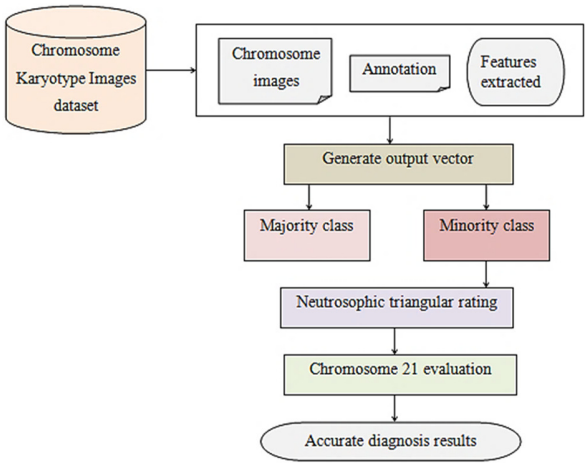

Fig. 5. Structure of the NEML-based classification model.

V. NEUTROSOPHIC EXTREME ML CLASSIFICATION

The proposed Neurotrosophic Extreme Machine Learning (NEML) model, shown in Figure 5, was used to improve prenatal identification of chromosomal abnormalities related to DS. Chromosome images, annotations, and extracted features are provided as inputs to the NEML classifier, which generates an output vector and separates samples into majority and minority classes. To address dataset imbalance, a Neutrosophic Bonferroni function with neutrosophic triangular rating assigns distinct weight values to samples, improving minority class classification compared to traditional Extreme ML that uses equal weights without fine-tuning.

The output of the ELM with l hidden nodes and activation function f is mathematically formulated as:

$$O_i = \sum_{k=1}^{L} \alpha_k f(W_k, B_k, x_k), \quad i = 1,2,..,n \quad (7)$$

where x_k is k-th input sample, W_k is the weight vector, B_k is the hidden node bias, and α_k is the output weight. O_i is the clustered output for n samples, assuming zero training error for fine-tuning.

The chromosome karyotype dataset used in this study exhibits significant class imbalance, where normal samples greatly outnumber abnormal samples. Specifically, the dataset contains 4893 normal samples and only 107 abnormal samples (57 numerical abnormalities and 50 structural abnormalities). Such an imbalance may bias traditional classifiers toward the majority class.

$$OV_i = \sum_{k=1}^{L} \alpha_k f(W_k, B_k, x_k), i = 1,2,..,n \quad (8)$$

Equation (8) shows that the output vector OV may be biased toward the majority class, leading to class imbalance, which is addressed using the Neurotrosophic Bonferroni function. By representing OV in a neutrosophic set with truth, falsity, and indeterminacy memberships, distinct weights are assigned to minority and majority class samples for balanced classification.

$$W^{min} = \frac{C_r}{T_A(OV)+I_A(OV)+F_A(OV)} \quad (9)$$

$$W^{maj} = \frac{1}{T_A(OV)+I_A(OV)+F_A(OV)} \quad (10)$$

where C_r denotes the ratio of the number of samples in the majority class, $T_A(OV)$ is the true area (or true pixels) in the overlapped region, $I_A(OV)$ is the incorrectly predicted area in the overlap, and $F_A(OV)$ is the false area or false prediction region.

The workflow of the proposed classification mechanism can be summarized as follows.

- Step 1 - Input Feature Vector: The extracted chromosome features obtained from the QC-based feature extraction stage are represented as an input vector

$$X = \{x_1, x_2, x_3, \ldots\ldots\ldots x_i\} \quad (11)$$

where x_i represents the extracted feature attributes of chromosome images.

- Step 2 - Identification of Majority and Minority Classes: N_{maj} denotes the number of majority samples and N_{min} denotes the number of minority samples.
- Step 3 - Class Imbalance Ratio: The imbalance ratio, calculated as given below, is used to determine the relative importance of minority class samples during classification.

$$R = \frac{N_{maj}}{N_{min}} \quad (12)$$

- Step 4 - Neurotrosophic Representation of the Output Vector: The ELM generates an output vector OV, which is represented using a neutrosophic set consisting of three membership functions: Truth membership T, Indeterminacy membership I, and Falsity membership F. This representation helps capture uncertainty in classification decisions.
- Step 5 - Application of Neurotrosophic Bonferroni Function: The Neurotrosophic Bonferroni function is applied to adjust the classification weights based on the imbalance ratio. The function assigns higher importance to minority class samples while reducing the dominance of majority class samples. This weighting mechanism improves the classifier's ability to detect abnormalities associated with chromosome 21 trisomy.
- Step 6 - Weighted ELM Classification: The weighted samples are used in the ELM model, where adaptive weights are assigned to training samples according to their neutrosophic membership values. The classifier then predicts the presence or absence of DS based on chromosome abnormalities.

$$R\big(T_A(OV), I_A(OV), F_A(OV)\big) = \frac{1}{2}\big(1 + T_A(OV) - 2 * I_A(OV) + F_A(OV)\big) \quad (13)$$

Using the obtained rating values, the output vector $OV = (OV_1, OV_2, OV_3)$—representing name, size, and box pixel values—is modeled through a single-valued neutrosophic triangular set to mathematically distinguish majority and minority class samples.

$$(Tn, In, Fn) = \big((Tn^U, In^U, Fn^U), (Tn^L, In^L, Fn^L)\big) \quad (14)$$

where Tn^U, In^U, Fn^U and Tn^L, In^L, Fn^L represent the upper (i.e., majority class) and lower (i.e., minority class) neutrosophic member function, forming the level set as:

$$(Tn^U_{OV}, In^U_{OV}, Fn^U_{OV})\big[R\big(Tn^U_1(OV), In^U_1(OV), Fn^U_1(OV)\big), R\big(Tn^U_2(OV), In^U_2(OV), Fn^U_2(OV)\big), \dots\big] \quad (15)$$

$$(Tn^L_{OV}, In^L_{OV}, Fn^L_{OV})\big[R\big(Tn^L_1(OV), In^L_1(OV), Fn^L_1(OV)\big), R\big(Tn^L_2(OV), In^L_2(OV), Fn^L_2(OV)\big), \dots\big] \quad (16)$$

These equations offer the upper (i.e., majority class) and lower (i.e., minority class) neutrosophic member function results. Since this study focuses on chromosome 21 to analyze and validate the presence/absence of DS, this chromosome is considered to be in the lower (i.e., minority class) neutrosophic member function, whereas the upper (i.e., majority class) deals with other chromosomes. So by discarding the majority class and retaining the minority class, the presence/absence of DS is determined by evaluating the results.

VI. EXPERIMENTAL SETUP

The proposed QC-NEML prenatal diagnosis model was implemented in Python on a Windows platform (i3-2350, 2 GB RAM) and evaluated using the dataset in [14], which consists of 5,000 samples. Performance was measured using precision, recall, accuracy, and misclassification rate. Several scientific computing libraries were utilized for model development and experimentation, including NumPy for numerical computations, OpenCV for image processing, and Scikit-learn for ML utilities. These libraries were employed for feature extraction, data handling, and performance evaluation. Finally, the results were compared against conventional methods, XGBoost [1] and AI-CK [2].

Before model training, the chromosome karyotype images underwent a preprocessing stage. In this stage, images were normalized and resized to ensure consistent dimensional representation. Annotation files, accompanying the dataset, were used to extract chromosome attributes such as bounding box coordinates and size parameters. These attributes were subsequently used in the QC feature extraction stage to construct feature vectors for classification. The processed feature vectors were then supplied to the NEML classifier for model training and evaluation.

To ensure reliable performance evaluation and avoid model bias due to dataset imbalance, a 10-fold cross-validation strategy was employed during the experimental analysis. In this approach, the complete dataset of 5000 chromosome karyotype images was randomly divided into 10 equal subsets (folds). In each iteration, nine folds were used for model training, while the remaining one was used for testing. This process was repeated ten times, such that each subset served as the testing set exactly once. The final performance metrics were obtained by averaging the results across all folds. This evaluation strategy helps improve the robustness of the results and reduces the possibility of overfitting during model training. Using cross-validation also ensures that both the majority (normal chromosomes) and minority classes (numerical and structural abnormalities) are proportionally represented in training and testing phases.

VII. RESULTS

A. Precision and Recall

Precision and recall were calculated using:

$$\text{Pre} = \frac{\text{TP}}{\text{TP+FP}} \quad (17)$$

$$\text{Rec} = \frac{\text{TP}}{\text{TP+FN}} \quad (18)$$

where TP denotes True Positives, FP denotes False Positives (FP), and FN denotes False Negatives. Figure 6 compares QC-NEML, XGBoost [1], and AI-CK [2] for DS prediction using 500–5000 karyotype images over 10 simulation runs. With 500 samples (350 DS, 150 non-DS), QC-NEML achieved higher

TP (340) and lower FP/FN (10/20) than XGBoost [1] (330, 20/30) and AI-CK [2] (300, 30/50). Accordingly, QC-NEML obtained superior precision (0.97) and recall (0.94) compared to XGBoost [1] (0.94, 0.91) and AI-CK [2] (0.85, 0.89). These improvements are attributed to the QC feature extraction and three-qubit mechanisms, reducing false positives by 8% and 17% and enhancing recall by 6% and 19% over the models in [1] and [2], respectively.

TABLE II. PRECISION MEAN AND SD ANALYSIS

	Precision		
	QC-NEML	**XGBoost [1]**	**AI-CK [2]**
Mean	0.923	0.857	0.791
SD	0.029	0.037	0.038

TABLE III. RECALL MEAN AND SD ANALYSIS

	Recall		
	QC-NEML	**XGBoost [1]**	**AI-CK [2]**
Mean	0.875	0.827	0.735
SD	0.046	0.049	0.067

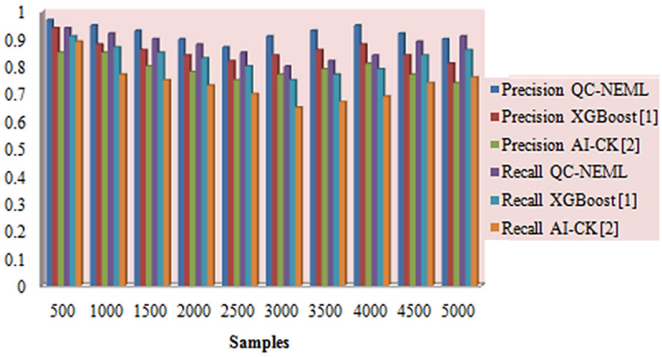

Fig. 6. Comparison of the precision and recall results.

B. Accuracy

The accuracy of prenatal diagnosis for detecting DS chromosome abnormalities was calculated using:

$$\text{Acc} = \frac{\text{TP+TN}}{\text{TP+TN+FP+FN}} \quad (19)$$

where TN represents True Negatives. Figure 7 presents the accuracy comparison for DS chromosomal abnormalities using QC-NEML, XGBoost [1], and AI-CK [2] over 10 cross-validation runs. For 500 samples (150 non-DS), true negatives were 130 for QC-NEML, 120 for XGBoost [1], and 115 for AI-CK [2]. Overall accuracy rates were 94%, 90%, and 83% for QC-NEML, XGBoost [1], and AI-CK [2], respectively. The superior performance of QC-NEML is attributed to the NEML algorithm and the Bonferroni-based neutrosophic set handling class imbalance. This approach improved TN, resulting in an accuracy improvement of 4.4% compared to XGBoost and 13.3% compared to AI-CK.

TABLE IV. ACCURACY MEAN AND SD ANALYSIS

	Accuracy (%)		
	QC-NEML	**XGBoost [1]**	**AI-CK [2]**
Mean	88.52	83.74	75.05
SD	3.13	3.35	3.72

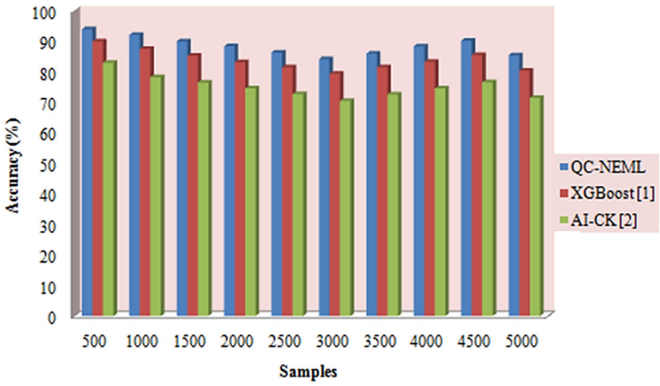

Fig. 7. Comparison of the accuracy results.

C. Performance Analysis of Misclassification Rate

The Misclassification Rate (MR) in prenatal DS diagnosis, calculated as the complement of the correct classification rate, measures the percentage of incorrectly classified sample images.

$$\text{MR} = \sum_{i=1}^{n} \frac{SI_{WC}}{SI_i} \quad (20)$$

is obtained by considering the sample images for simulation SI_i and the sample images wrongly classified and diagnosed SI_{WC}. MR is measured in terms of percentage (%).

Figure 8 shows the misclassification rates of QC-NEML, XGBoost [1], and AI-CK [2] over 5000 sample images across 10 cross-validation runs. QC-NEML outperforms the other models, reducing misclassification by 21% compared to [1] and 35% compared to [2], due to its NEML approach. This method evaluates feature weights, applies neutrosophic functions, and focuses on chromosome 21, improving classification accuracy.

TABLE V. MISCLASSIFICATION RATE MEAN AND SD ANALYSIS

	Misclassification rate (%)		
	QC-NEML	**XGBoost [1]**	**AI-CK [2]**
Mean	4.53	5.76	6.93
SD	0.42	0.56	0.63

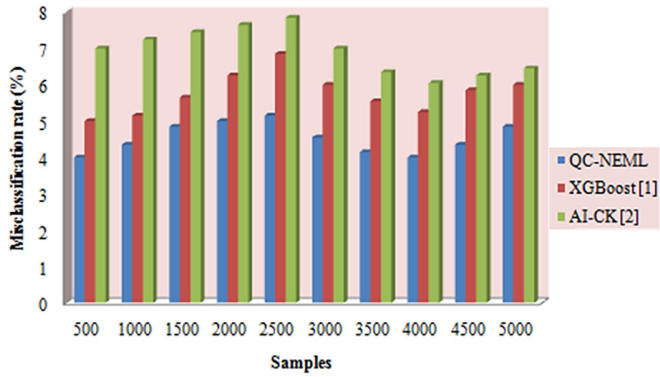

Fig. 8. Comparison of the misclassification rate analysis.

D. Statistical Validation of Results

To further evaluate the robustness of the proposed QC-NEML model, statistical validation was performed across the ten simulation runs. The performance metrics, including precision, recall, accuracy, and misclassification rate, were analyzed by computing their mean and standard deviation values. Let M_i denote the value of a performance metric obtained in the i-th simulation run and n denote the total number of runs. The mean value of the metric is calculated as

$$\mu = \frac{1}{n}\sum_{i=1}^{n} M_i \quad (21)$$

The corresponding standard deviation is computed as

$$\sigma = \sqrt{\frac{1}{n-1}\sum_{i=1}^{n}(M_i - \mu)^2} \quad (22)$$

where μ represents the average performance across simulation runs and σ indicates the variability of the results. The results in Tables II-IV show better means and lower standard deviation values for the proposed QC-NEML model, indicating that it produces consistent results across multiple runs. The statistical analysis confirmed that the proposed model demonstrated stable and superior performance in detecting chromosomal abnormalities associated with DS.

Recent studies show that CNN-based deep learning models effectively detect chromosome abnormalities by learning complex visual patterns from karyotype images. However, these models require large annotated datasets and high computational resources. The proposed QC-NEML model offers a lightweight alternative using quantum-inspired feature extraction with NEML, with future work aiming to integrate deep learning features and benchmark against CNN models.

VIII. CONCLUSION

DS arises due to the trisomy of chromosome 21 and remains one of the most frequently occurring chromosomal disorders affecting human development. Karyotyping analyzes the number and structure of chromosomes to detect abnormalities related to DS. Early prediction of DS has gained significant interest in the research community. This study proposes a QC-NEML method for the prenatal diagnosis of chromosomal abnormalities. The method combines QC-based feature extraction with NEML classification for DS prediction. The integration of these components improves the efficiency and accuracy of the QC-NEML method in detecting DS. The experimental results demonstrate that QC-NEML outperforms conventional DS diagnosis methods, achieving 94% classification accuracy, outperforming XGBoost and AI-CK methods by 4.4% and 13.3% in accuracy, respectively. Furthermore, the misclassification rate is reduced by 40% and 65%, respectively, demonstrating the effectiveness of the proposed method in detecting chromosomal abnormalities associated with DS.

DECLARATION OF COMPETING INTERESTS

The authors declare no competing interests that could have influenced the results of this work.

ACKNOWLEDGMENT

The authors would like to thank all individuals and institutions who supported this work.

DATA AVAILABILITY

The data that support the findings of this study are publicly available in [14].

AI USE AND DECLARATION OF GENERATIVE AI USE

During the preparation of this manuscript, ChatGPT was utilized in rephrasing certain sentences. All generated content was carefully reviewed and edited as necessary, and the author takes full responsibility for the accuracy and integrity of the final manuscript.

REFERENCES

[1] H. D. Do *et al.*, "Applying machine learning in screening for Down Syndrome in both trimesters for diverse healthcare scenarios," *Heliyon*, vol. 10, no. 15, Aug. 2024, https://doi.org/10.1016/j.heliyon.2024.e34476.

[2] Y. Zhou *et al.*, "Enhancing chromosomal analysis efficiency through deep learning-based artificial intelligence graphic analysis," *Discover Applied Sciences*, vol. 6, no. 6, May 2024, Art. no. 299, https://doi.org/10.1007/s42452-024-05980-5.

[3] L. Hixson *et al.*, "An Overview on Prenatal Screening for Chromosomal Aberrations," *Journal of Laboratory Automation*, vol. 20, no. 5, pp. 562–573, Oct. 2015, https://doi.org/10.1177/2211068214564595.

[4] K. Nandhini and G. Tamilpavai, "An Optimal Stacked ResNet-BiLSTM-Based Accurate Detection and Classification of Genetic Disorders," *Neural Processing Letters*, vol. 55, no. 7, pp. 9117–9138, Dec. 2023, https://doi.org/10.1007/s11063-023-11195-3.

[5] R. A. Marnani, R. Jaros, J. Pavlicek, R. Martinek, and R. V. Kahankova, "Advancements and Challenges in Non-Invasive Electrocardiography for Prenatal, Intrapartum, and Postnatal Care: A Comprehensive Review," *IEEE Access*, vol. 12, pp. 44730–44747, 2024, https://doi.org/10.1109/ACCESS.2024.3378747.

[6] G. S. Kadakol, I. Bagoji, S. V. Patil, and R. S. Bulagouda, "Cytogenetic Analysis of Down Syndrome," *International Journal of Clinical and Biomedical Research*, pp. 37–40, Jan. 2019, https://doi.org/10.31878/ijcbr.2018.51.10.

[7] F. He, B. Lin, K. Mou, L. Jin, and J. Liu, "A machine learning model for the prediction of down syndrome in second trimester antenatal screening," *Clinica Chimica Acta*, vol. 521, pp. 206–211, Oct. 2021, https://doi.org/10.1016/j.cca.2021.07.015.

[8] Y. Abukhaled, K. Hatab, M. Awadhalla, and H. Hamdan, "Understanding the genetic mechanisms and cognitive impairments in Down syndrome: towards a holistic approach," *Journal of Neurology*, vol. 271, no. 1, pp. 87–104, Jan. 2024, https://doi.org/10.1007/s00415-023-11890-0.

[9] M. Nagaya and N. Ukita, "Embryo Grading With Unreliable Labels Due to Chromosome Abnormalities by Regularized PU Learning With Ranking," *IEEE Transactions on Medical Imaging*, vol. 41, no. 2, pp. 320–331, Oct. 2022, https://doi.org/10.1109/TMI.2021.3126169.

[10] F. Baldo *et al.*, "Machine learning based analysis for intellectual disability in Down syndrome," *Heliyon*, vol. 9, no. 9, Sept. 2023, https://doi.org/10.1016/j.heliyon.2023.e19444.

[11] I. N. Margret, K. Rajakumar, K. V. Arulalan, S. Manikandan, and Valentina, "Statistical Insights Into Machine Learning-Based Box Models for Pregnancy Care and Maternal Mortality Reduction: A Literature Survey," *IEEE Access*, vol. 12, pp. 68184–68207, 2024, https://doi.org/10.1109/ACCESS.2024.3399827.

[12] A. Asim, A. Kumar, S. Muthuswamy, S. Jain, and S. Agarwal, "Down syndrome: an insight of the disease," *Journal of Biomedical Science*, vol. 22, no. 1, June 2015, Art. no. 41, https://doi.org/10.1186/s12929-015-0138-y.

[13] A. Arjmand and N. Giannakeas, "Fat Quantitation in Liver Biopsies Using a Pretrained Classification Based System," *Engineering, Technology & Applied Science Research*, vol. 8, no. 6, pp. 3550–3555, Dec. 2018, https://doi.org/10.48084/etasr.2274.

[14] "Chromosome karyotype images." Kaggle, [Online]. Available: https://www.kaggle.com/datasets/aliabedimadiseh/chromosome-image-dataset-karyotype.